Effects of annealing on hydrogen microstructure in boron-doped and undoped rf-sputter-deposited amorphous silicon

S. Mitra and K. K. Gleason*
Department of Chemical Engineering, Massachusetts Institute of Technology, Cambridge, Massachusetts 02139

H. Jia and J. Shinar
Ames Laboratory and Physics and Astronomy Department, Iowa State University, Ames, Iowa 50011
(Received 28 December 1992)

A detailed study of changes in hydrogen microstructure in rf-sputter-deposited undoped and boron-doped hydrogenated amorphous silicon was undertaken. The boron-doped samples were prepared under identical conditions with the same hydrogen content, and then characterized by IR absorption and ^{1}H NMR before and after annealing. It is found that an increase in the boron concentration leads to increased segregation of hydrogen. Annealing leads to evolution of the hydrogen microstructure. This change, however, depends on the boron content of the films. After a moderate anneal, the hydrogen microstructure is found to evolve to the same state and seems to be independent of the boron content of the films.

I. INTRODUCTION

A. Background

Hydrogenated amorphous silicon (*a*-Si:H) is a technologically important material that is used in a wide variety of electronic devices such as solar cells, large-area image sensors, and thin-film transistors for liquid-crystal displays. The addition of hydrogen to amorphous silicon has several beneficial effects. First, hydrogen terminates unsaturated dangling bonds, thus removing unwanted electronic states that act as recombination centers from the energy gap. Second, the addition of hydrogen increases the band gap of the material and produces sharper band tail edges.[1] Device-quality hydrogenated amorphous silicon (*a*-Si:H) has an optical band gap of ~ 1.75 eV and a paramagnetic defect density of less than 10^{16} cm^{-3}.[2] Also, *a*-Si:H has a high ratio of photoconductivity to dark conductivity, typically greater than 10^5, making it an attractive material for application in solar cells[2] and thin-film transistors.[3] However, a major problem with *a*-Si:H remains the generation of light-induced metastable defects which lead to the degradation of the material during its use.[4,5] The mechanism of this so-called Staebler-Wronski effect is poorly understood. It is now generally thought that these light-induced defects and hydrogen microstructure are closely linked.[6–10] Consequently, a better understanding of the hydrogen microstructure is necessary to further improve the electronic quality of the material.

^{1}H nuclear magnetic resonance (NMR) is a powerful technique to study hydrogen microstructure. Previous studies have established that hydrogen is bonded inhomogeneously in *a*-Si:H.[11–14] The Fourier transform of the free induction decay (FID) typically contains two components corresponding to the two distinct hydrogen bonding environments. The narrow Lorentzian is predominantly attributed to hydrogen in the isolated (or dilute) phase, while the broad Gaussian is associated with hydrogen in the clustered phase. A third configuration of trapped H_2 molecules constitutes only a small fraction of the narrow line. This H_2 can be indirectly detected through the spin-lattice relaxation time T_1 which increases with decreasing H_2 concentration.[11] A precise description of the clustered phase is more difficult. A ^{1}H is assumed to be in a "clustered" environment if it experiences a significant dipole-dipole interaction (>1 kHz) from its neighboring protons. Consequently, the size of these hydrogen clusters can be probed directly by ^{1}H multiple quantum (MQ) NMR measurements.[12,14]

MQ NMR measurements on device-quality glow-discharge-deposited *a*-Si:H films have shown that a typical cluster contains 5–7 hydrogen atoms. As the hydrogen content in the films increases, the number of such clusters increases, and finally at high enough hydrogen concentration, distinct small clusters are no longer apparent.[14] Hydrogen in an isolated phase or in a H_2 molecule which contributes to the narrow component of the two-component FID is not expected to be observed in the MQ NMR experiments.

Since the chemical shift difference between ^{1}H in $-SiH_2$ and $-SiH_3$ is small, and the linewidths associated with the clustered hydrogen are broad (~ 25–30 kHz full width at half maximum), ^{1}H NMR cannot be used to resolve these two bonding configurations.[15] Information on the bonding configuration can, however, be obtained from the infrared (IR) absorption. The total hydrogen content $[H_t]_0$ and the concentration of hydrogen in the $-SiH_2$ and $-SiH_3$ configuration N_{d0} was determined from the 640 cm^{-1} wagging and 840–890 cm^{-1} scissors mode, respectively. The interpretation of the stretching mode (2000–2100 cm^{-1}), however, is more complicated.[16,17] A peak at 2000 cm^{-1} is generally attributed to bulk hydrogen in the *a*-Si:H bonding configuration residing in the isolated phase. However, the frequency of a mono-H stretch mode increases from 2000 to 2100 cm^{-1}

 ©1993 The American Physical Society

as the radius of the void around the H increases to 2 Å.[18] However, hydrogen residing on the inner surfaces of highly compact disklike microvoids with opposing surfaces ≤ 3 Å will experience screening similar to that in the bulk and consequently vibrate at 2000 cm^{-1}.[19] The peak at 2100 cm^{-1} has been attributed to both silicon bonded to multiple hydrogen atoms, as well as to clusters of silicon atoms each bonded to one hydrogen atom.[20] Correlation of MQ NMR results with IR data have been used to attribute the stretch frequency of 2080 cm^{-1} to these clusters.[14] Thus, the stretching peak is not considered to be a reliable indicator of the hydrogen bonding configuration in *a*-Si:H.

It has been reported that in glow-discharge (gd) deposited boron-doped films, some hydrogen irreversibly converts from bulk mono-H to $-SiH_2$ and $-SiH_3$ configurations during annealing at 200 °C.[21] Thus even moderate annealing of boron-doped films results in changes in the Si network consistent with the rise in microvoid-related hydrogen content. These processes were faster in *p*-type than in *n*-type films. Since hydrogen diffusion is the fastest in boron-doped films, it appears to be controlling the above changes and the consequent evolution of the hydrogen microstructure. Thus, in this paper, we have studied the effect of boron concentration on hydrogen microstructure in boron-doped rf-sputter-deposited *a*-Si:H. Hydrogen diffusion experiments in rf-sputter-deposited undoped and boron-doped *a*-Si:H has established the existence of deep trapping sites that render hydrogen immobile.[6,16,22] Though the nature of these sites has not yet been unambiguously established, it has been suggested that flat disk-shaped microvoids, as described above, are indeed these deep traps.[6] Since hydrogen atoms residing in these sites are in close proximity, they experience dipole-dipole interaction and can be thought of as "clustered." Consequently, ^1H NMR studies have been combined with IR measurements in order to investigate the hydrogen dynamics in both as-deposited and annealed films.

B. Multiple quantum (MQ) NMR theory

MQ NMR is a powerful technique that has been widely used to probe the dynamics of a group of interacting nuclei. Since there is a considerable amount of literature describing the theory and implementation of MQ NMR, only a brief description will be presented here.[14,23–25]

MQ NMR is a two-dimensional experiment where a group of N interacting spin $\frac{1}{2}$ nuclei are correlated through their dipole-dipole interaction. The experiment itself consisted of four distinct periods called the preparation, evolution (which in our case was set to zero), mixing, and detection. The preparation cycle consists of a total of eight 90° pulses—four x pulses followed by four $-x$ pulses. The average Hamiltonian for the homonuclear couplings H_{yx} is given by

$$H_{yx} = -\tfrac{1}{2} \sum_{i<j} D_{ij}(I_{i+}I_{j+} + I_{i-}I_{j-}) , \quad (1)$$

where D_{ij} is the dipolar coupling constant between spins i and j and I_+ and I_- are the well-known raising and lowering operators. The presence of the bilinear raising and lowering operators ensures the coherent superposition of states such that $n = 0, \pm 2, \pm 4, \ldots, \pm N$, corresponding to simultaneous transitions of $0,2,4,\ldots,N$ spins. Here n is called the order of the multiple quantum coherence and represents the change in magnetization in the z direction. The evolution of the N-interacting spin system is described by the Liouville–von Neumann equation

$$\frac{d\rho(\tau)}{d\tau} = i[\rho(\tau), H_{yx}] , \quad (2)$$

where $\rho(\tau)$ is the density matrix at time τ, since each spin can yield both up (α) or down (β) eigenstates with respect to the applied magnetic field. $\rho(\tau)$ is a $2^N \times 2^N$ matrix of the resultant product states. At equilibrium, the density matrix is proportional to I_z and only the principal diagonal has nonzero elements representing the population in those states. Each off-diagonal element of the density matrix correlates transitions between two states. The number of states having a multiple quantum coherence of order n, Z_n is then given by

$$Z_n = \binom{2N}{N-|n|} \approx 4^N (\pi N)^{-1/2} e^{-n^2/N} \quad \text{for } N > 6 . \quad (3)$$

As the sample is subjected to the pulse sequence during the preparation period, intensities in the off-diagonal elements begin to develop. After sufficiently long excitation times, elements far off the diagonal develop significant intensity. Eventually the statistical limit is reached where all allowed MQ coherences have become equally likely. Thus the intensity of a particular MQ transition of order n simply becomes proportional to Z_n,

$$I(n,\tau) \sim \exp[-n^2/N(\tau)] ,$$

where $N(\tau)$ is the effective number of correlated spins at preparation time τ. Information on ^1H distribution is obtained by increasing τ and monitoring the variations in $N(\tau)$, the "effective cluster size." If the number of spins in a cluster is finite, $N(\tau)$ saturates at long τ. On the other hand, for an "infinite" cluster size $N(\tau)$ would increase continuously with time without any upper bound. Here "infinite" indicates the cluster length scale is greater than that of the MQ experiment, which is generally ~ 20 Å.

II. EXPERIMENTAL DETAILS

The samples studied in this work were deposited by rf sputtering of a high-purity polycrystalline silicon target at a transmitter power of 600 W held in a mixture of 10 mTorr of argon, 0.3 mTorr of hydrogen, and up to 1.6 mTorr of a 99% argon, 1% diborane mixture. The boron content of the films was determined by secondary-ion mass spectrometry (SIMS) by comparing the boron counts from the samples with that of a standard.[6,17] Samples deposited on the silicon wafer were used for IR absorption, which was performed on a single-beam Fourier transform infrared (FTIR) spectrometer IBM model IR 98. The total hydrogen content [H_t] and the concentration of hydrogen in $-SiH_2$ and $-SiH_3$ bonding configurations were obtained from the 640 cm^{-1} wagging and 840–890 cm^{-1} scissors mode, respectively. The

number density N of oscillators in each vibrational mode was determined from the relation

$$N = A^* \int \frac{\alpha(\omega)}{\omega} d\omega \ , \tag{4}$$

where $\alpha(\omega)$ is the absorption coefficient, ω is the angular frequency, and A^* is a proportionality constant. Following the suggestion of Shanks *et al.*,[26] the values of A^* used in this work were 1.6×10^{19} cm^{-2} and 2×10^{20} cm^{-2} for the wagging and scissors mode, respectively.

The films for NMR analysis were deposited on aluminum foils which were subsequently etched away in dilute HCl. The ^{1}H MQ NMR experiments were performed on a home-built 270-MHz spectrometer with a variable phase synthesizer. Each preparation subcycle lasted 60 μs and consisted of eight 2.2 μs $\pi/2$ pulses. The mixing cycle is identical to the preparation cycle with the x and $-x$ replaced by y and $-y$ pulses and results in time reversal. The phase of the preparation sequence was varied from 0 to 2π in 32 increments and the corresponding plot of signal intensity was Fourier transformed to yield the MQ intensities $I(n,t)$. A 1-ms delay after the mixing period ensured the destruction of the transverse magnetization prior to the detection pulse. The spin-lattice relaxation-time constant T_1 was determined using the usual saturation recovery method.[27] All NMR experiments were done at room temperature.

III. RESULTS AND DISCUSSION

The results of the SIMS and IR absorption measurements undertaken on three as-deposited films, labeled 1 through 3, are summarized in Table I. The boron concentration varied within the samples with sample 1 having the maximum concentration (1.5×10^{20} cm^{-3}), while sample 3 was intrinsic. The total hydrogen content [H_T] in both samples 1 and 2 was determined to be $\sim7.0\pm1.0$ at. %, while sample 3 contained ~15 at. % of hydrogen. The total concentration of hydrogen bonded in the $-SiH_2$ and $-SiH_3$ type of configuration N_{d0} varied from sample to sample. While the stretching mode in sample 2 showed a single sharp peak at 2000 cm^{-1}, both samples 1 and 3 exhibited an additional peak at ~2100 cm^{-1}. Note that the latter samples also had some hydrogen bonded in the $-SiH_2$ and $-SiH_3$ configuration as seen from the scissors mode between 840–890 cm^{-1}.

The ^{1}H NMR results on both as-deposited and annealed samples are shown in Table II, which shows changes in the spin-lattice relaxation-time constant T_1, the fraction of the intensity of the broad component f_B, and the second moment M_2 upon annealing. The spin-lattice relaxation-time constant T_1, of the rf-sputter-deposited film (sample 3) is similar to that of intrinsic films deposited by glow-discharge processes,[28] while the doped materials (samples 1 and 2) have longer T_1 values. For these samples the number of spins correlated after a preparation time $N(\tau)$, as measured from the MQ NMR experiments, is shown in Fig. 1. As expected, $N(\tau)$ increases with increasing preparation time. The magnitude of the $n=1$ coherence (which is a measure of noise in this spectrum) also grows with preparation time, limiting the experiments to $\tau\leq720$ μs.

Since the total hydrogen content in samples 1 and 2 are the same, the effect of boron concentration on hydrogen microstructure can be directly compared with each other. Care should be taken in comparing the MQ NMR results of the doped and the intrinsic films since the hydrogen contents are different. It appears from Fig. 1 that the number of spins correlated at long preparation times is about the same in both samples 1 and 2. While in sample

TABLE I. Characteristics of as-deposited samples.

Sample No.	[B] (cm^{-3})	[H_T]$_0$ at. %	N_{d0} at. %	Stretch peak (cm^{-1})
1	1.5×10^{20}	7.6	1.4	2000, 2128
2	8.0×10^{18}	7.0		2000
3	undoped	15.0	3.5	2004, 2098

TABLE II. Annealing steps and characterization of the samples by ^{1}H NMR after each anneal.

Sample No.	Annealing steps Temp. (°C)	Time (h)	f_B	T_1 (s)	$M_2^{1/2}$ (kHz)
1	as-deposited		0.40	25	11.2
	155	2.0	0.45	26	11.4
		11.25	0.34	22	8.5
	220	10.25	0.40	24	9.4
2	as-deposited		0.67	20	8.5
	155	2.0	0.38	38	12.4
		11.25	0.23	35	13.7
	220	9.88	0.38	39	10.5
3	as-deposited		0.66	8	12.1
	335	7.0	0.66	10	14.2

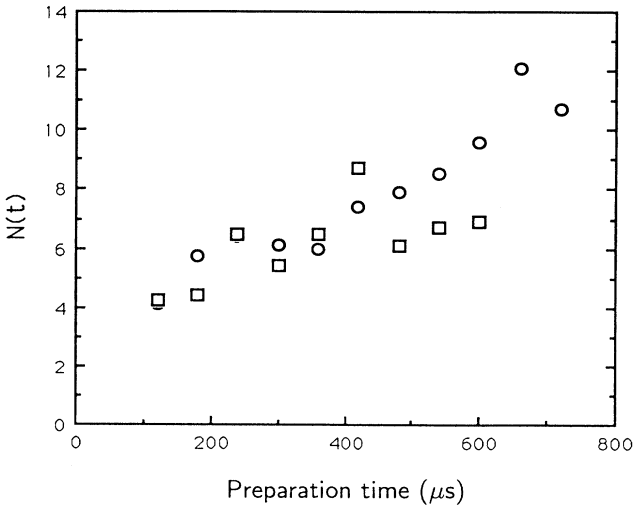

FIG. 1. Spin-correlation growth with preparation time in the as-deposited boron-doped samples. Note that sample 1 (circles) is more heavily doped than sample 2 (squares).

1, $N(\tau)\sim 9\pm 1$ spins at $\tau=600$ μs, $N(\tau)$ stays roughly constant at 7 ± 1 spins for $240\leq\tau\leq 600$ μs in sample 2, suggesting that a typical cluster contains 6–10 hydrogen atoms with little or no intercluster dipolar communication. These numbers are in general agreement with glow-discharge-deposited intrinsic a-Si:H with similar hydrogen content.[14] This is not surprising because the hydrogen microstructure is expected to be primarily determined by the total hydrogen content and hydrogen mobility during growth (and hence substrate temperature). Although these samples were not separately heated during growth, the substrate temperature at 550 W is estimated to be 180 °C,[6] and is thus comparable to that of glow-discharge films.

Another interesting feature in these results is that although the number of spins correlated at $\tau=600$ μs is about the same in both samples (Fig. 1), f_B, the fraction of hydrogen contributing to the broad component, is considerably larger in sample 2. However, its IR exhibits a clear, sharp peak at 2000 cm^{-1} and no discernible absorption between 840–890 cm^{-1}, suggesting little or no hydrogen bonded in the $-SiH_2$ and $-SiH_3$ type of configuration. Thus in sample 2, hydrogen contributing to the 2000 cm^{-1} stretch peak also contributes to the broad component through homonuclear dipole interactions and participates in the MQ transitions, suggesting that some of the hydrogen vibrating in this frequency is in a clustered phase.

The effect of annealing on hydrogen distribution in the samples was also investigated in detail. Samples 1 and 2 received four successive anneals. The first anneal was for 2 h at 155 °C followed by an additional 9-h anneal. A final anneal for $\sim$10 h was performed at 220 °C. Sample 3, being intrinsic, is expected to have a lower hydrogen diffusion constant than its doped counterparts,[6,16,22] and was annealed at a relatively higher temperature of 335 °C. After each anneal step the sample were characterized by both IR and NMR.

The IR absorption showed that there was little or no loss of hydrogen during each stage of anneal. However, the NMR results did show changes that depend on the boron concentration and are shown explicitly in Table II. Although changes were observed in the values of T_1, f_B, and the linewidths of the Gaussian component upon annealing at 155 °C, there was little or no effect on the H distribution as measured from the MQ NMR experiments. This is demonstrated in Fig. 2, which shows the growth of spin-correlation size with τ. Though the data for sample 1 show some fluctuations, neither show any significant changes in the hydrogen cluster size. This is to be expected since both hydrogen diffusion and structural relaxations at this temperature are slow.[6,16,22] However, the value of T_1 increases even after this moderate anneal at 155 °C. Since trapped H_2 molecules act as ^{1}H spin-lattice relaxation centers,[11] this implies a loss of H_2 molecules. Consequently, this change of T_1 is not expected to be indicative of hydrogen microstructural changes. However, f_B remained virtually unchanged in sample 1 while it decreased upon moderate annealing in sample 2. This suggests some change in the hydrogen bonding environment which the MQ NMR, however, was unable to pick up.

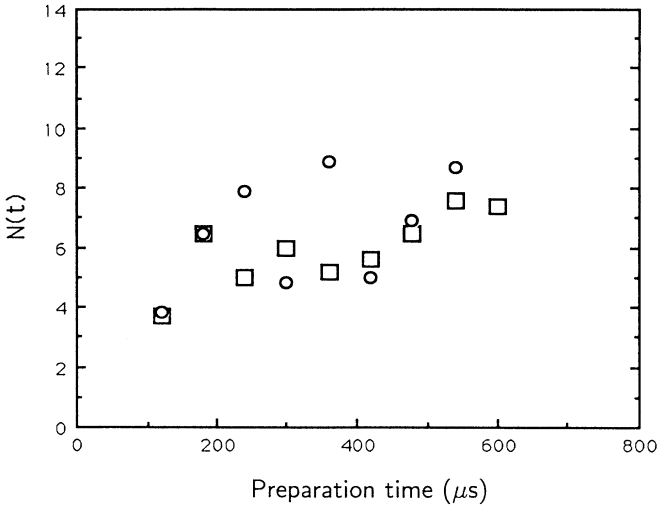

FIG. 2. Spin-correlation size with preparation time after an anneal at 155 °C for 11.25 h in sample 1 (circles) and sample 2 (squares). Though $N(\tau)$ shows some scatter in sample 1, the number of spins correlated at $\tau\sim 600$ μs remains approximately the same in both samples.

Thus in order to detect changes in the size of the hydrogen clusters in these samples, it was necessary to anneal them at higher temperatures at which hydrogen diffusion become significant. Once again the dependence of the spin-correlation size $N(\tau)$ on the preparation time τ after a $\sim$10-h anneal at 220 °C is shown in Fig. 3. Where reliable values can be achieved out to 1000 μs, the number of correlated spins seems to level off at 11 ± 1 atoms. While the hydrogen cluster size remains roughly the same in sample 1, it seems to increase in sample 2. However, it should be noted that most of the spin-correlation measurements in this sample were limited to $\tau\leq 600$ μs.

Sample 3, being intrinsic, was annealed at an even higher temperature of 335 °C for 7 h. The dependence of the spin-correlation size on τ both before and after annealing is plotted in Fig. 4. It is clear that for the annealed sample $N(\tau)$ increases without an upper bound, indicating hydrogen cluster sizes much bigger than its doped counterpart. Since it contains twice the amount of hydrogen than its doped counterparts, care should be exercised in comparing the two sets of data.

In order to gain a better insight on the hydrogen distribution, the spin-correlation size for the annealed sample is replotted in Fig. 5 against the scaled, dimensionless preparation time $M_2^{1/2}\tau$. One measure of the dipolar field strength is the square root of the second moment $M_2^{1/2}$. After accounting for the strength of the dipole-dipole interaction, the rate at which spins are correlated would now depend on the number of nearest neighbors.[29] Since this is a strong function of the dimensionality of the spin distribution, the growth rate is expected to be fastest in three-dimensional distributions and the slowest in one-dimensional systems.[29] The growth rate of the spins in sample 3 has been compared with that from calcium hy-

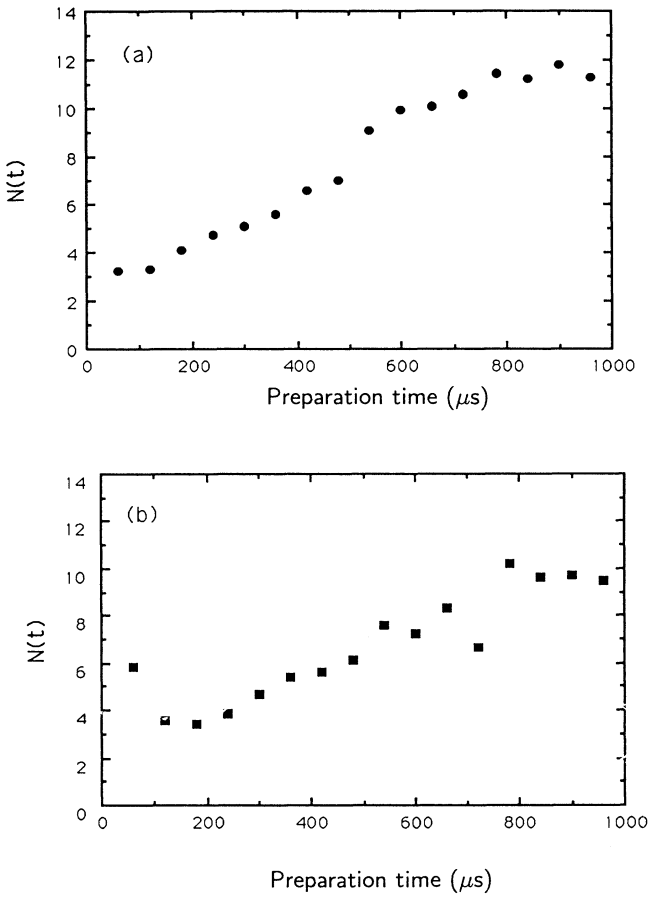

FIG. 3. $N(\tau)$ vs τ after an anneal at 220 °C for ~10 h for (a) sample 1 and (b) sample 2. Note that the number of spins correlated at levels of ~9–12 for both samples.

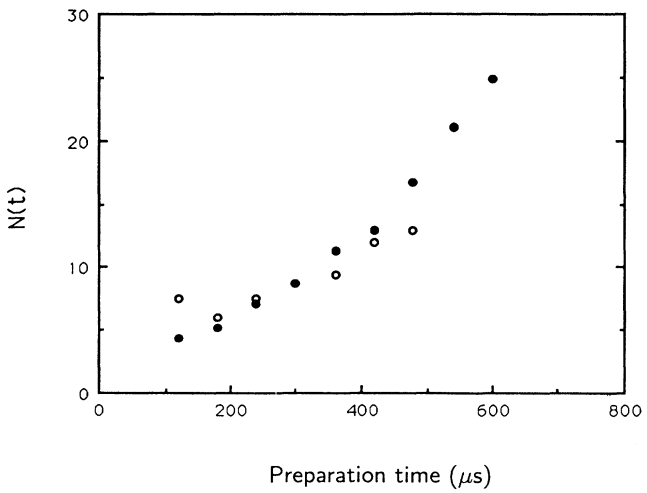

FIG. 4. $N(\tau)$ vs τ for sample 3 before (open circles) and after an anneal at 335 °C for 7 h (solid circles). Note that the number of spins correlated after annealing increases without an upper bound, indicating an infinite cluster size.

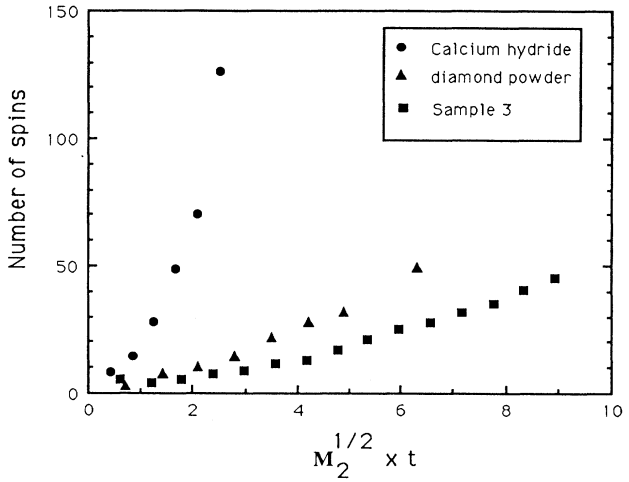

FIG. 5. Rate of growth of the spin-correlation size vs scaled preparation time. Note that the growth rate is slowest in sample 3.

dride ($M_2^{1/2}=11.6$ kHz) and hydrogenated surface natural diamond powder (with particle sizes <0.1 μm, $M_2^{1/2}=19.5$ kHz), which were considered to be model three- (bulk) and two- (surface) dimensional distributions of hydrogen, respectively. As expected, the growth rate is faster in calcium hydride than for the hydrogenated diamond surfaces. However, the slowest growth rate is seen for sample 3. This indicates that the dimensionality of the hydrogen distribution in this intrinsic *a*-Si:H sample is less than two. This result is consistent with the fact that rf-sputtered "hydrogen-rich" samples ($[H_T]>10$ at. %) exhibit columnar morphology with much of the hydrogen residing on the inner surfaces of columns.[6] The distribution of hydrogen in this sample is thus expected to be nearly two dimensional in nature.

It is also instructive to compare the $N(\tau)$ in samples 1 and 2 with that of CaH_2 and diamond powder. While at $M_2^{1/2}\tau=3$ well over 100 spins are correlated in CaH_2, about 50 and 30 spins are correlated at $M_2^{1/2}\tau=7$ in natural diamond powder and sample 3, respectively. On the other hand, only 9–12 spins are correlated at $M_2^{1/2}\tau=7$ in both doped samples, providing additional support to the fact that the hydrogen clusters in these samples are isolated since MQ coherence growth is slow among a finite number of nuclei.

Another method of detecting changes in the microstructure is by comparing the intensities of the various orders in the MQ spectra. As has been mentioned earlier in this paper, at equilibrium only the diagonal states in the density matrix $\rho(t)$ have nonzero elements. Intensity in the off-diagonal elements develops as higher-order transitions are excited during the application of the preparation cycle. All ^1H nuclei, whether in the isolated or clustered phase, contribute to the intensity of the zeroth order $I(0)$. Thus the intensity of the zeroth order at any time τ may be written as $I(0,\tau)=I_{cl}(0,\tau)+I_{iso}(0,\tau)$, where $I_{cl}(0,\tau)$ and $I_{iso}(0,\tau)$ are the intensities from the clustered and the isolated phases, respectively.

However, only those hydrogen in the clustered phase can take part in the nonzero MQ transitions that contribute to the intensity of the higher orders. Thus the fraction of hydrogen taking part in nonzero MQ transitions at time τ, $M(\tau)$ can be defined as

$$M(\tau)=\frac{I_{\rm cl}(0,\tau)+\sum_{n=1}^{\infty}2I(2n,\tau)}{\sum_{n=0}^{\infty}I(2n,\tau)} . \quad (5)$$

The factor of 2 in the second term of the numerator is included in order to account for the negative MQ orders. As higher-order transitions are excited, $M(\tau)$ increases with increasing preparation time and finally saturates. Figure 6 shows the dependence of $M(\tau)$ on τ for the doped samples both before and after annealing. The value of $M_{\rm sat}$, the saturated value of M, is thus a measure of the fraction of hydrogen undergoing MQ transitions and is indicative of at least two ^{1}H nuclei in close proximity. Note that $M(\tau)$ begins to decrease slowly at longer values of τ for the annealed samples. This behavior is probably due to the relaxation of some of the higher MQ orders.

It is clear from Fig. 6 that although $[H_T]$ is comparable in both samples 1 and 2, the fraction of hydrogen undergoing MQ transitions is greater in sample 1. There is, however, another striking dissimilarity between the two samples. In sample 1, $M_{\rm sat}\sim 0.8$, which is twice the value of f_B, the fraction of total hydrogen contributing to the broad line. On the other hand, the situation in sample 2 is quite the opposite, where the values of f_B and $M_{\rm sat}$ are 0.67 and 0.45, respectively. The effect of annealing at 220 °C for $\sim$10 h on the value of $M_{\rm sat}$ is also shown in Fig. 6. Note that after this anneal both f_B and $M_{\rm sat}$ for the two samples are in close agreement to each other.

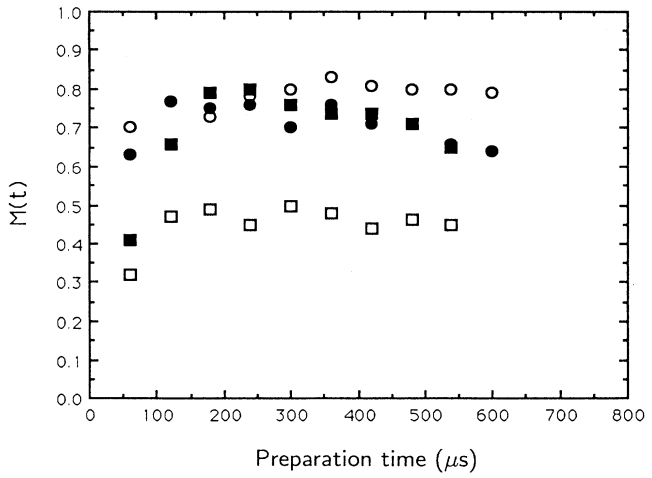

FIG. 6. Fraction of hydrogen taking part in MQ transitions M vs preparation time τ. Samples 1 and 2 are represented by circles and squares, respectively. The open symbols represent as-deposited samples, while the solid symbols represent annealing at 220 °C for $\sim$10 h. Note that $M(\tau)$ approaches similar values after annealing.

The effect of annealing on $I(n)$, the MQ intensities of order n, is shown in Fig. 7. As expected, the higher orders grow at the expense of $I(0)$ with increasing preparation time. The effect of relaxation of $I(2)$ is clearly seen for $t\geq 400$ μs. As $I(2)$ relaxes back to $I(0)$, its intensity decreases while there is a corresponding increase in $I(0)$. Several features in the data are worth noting. The two as-deposited samples show markedly different behavior. For the as-deposited samples, $I(n)$ $(n\geq 2)$ is consistently larger in sample 1, indicating that a larger fraction of hydrogen is taking part in each of these transitions. Upon annealing at 220 °C for $\sim$10 h, the values of $I(n)$ approach similar values, indicating that both samples relax to the same final state—a fact that is reflected by similar values of $M_{\rm sat}$ (Fig. 6) and $N(\tau)$ at $\tau\geq 800$ μs (Fig. 3).

Since the doped samples were deposited under identical conditions, the size and distribution of microvoids are expected to be the same. The diffusion of hydrogen in *a*-Si:H has been shown to increase with increasing boron concentration.[28,30] Consequently, the surface mobility of hydrogen during film growth is expected to be greater in sample 1 than in sample 2. Using the values quoted by Street *et al.*,[30] the diffusion of hydrogen in sample 1 is expected to be an order of magnitude greater than in sample 2. Thus, due to its enhanced mobility, hydrogen passivates most of the deep trapping sites in sample 1 during deposition. Since these sites are thought to be disk-shaped microvoids with opposing surfaces ≤ 3 Å apart, the hydrogen atoms residing in these traps are in close proximity to each other and experience dipolar interaction. Though this hydrogen would participate in MQ transitions, $N(\tau)$ ultimately levels off, corresponding to the average number of hydrogen atoms that can be accommodated in these sites.

A number of studies have also shown that the presence of dopants in the bulk of crystalline silicon leads to the formation of dopant-hydrogen complexes.[31–33] For example, Pankove *et al.*[31] have suggested the formation of a bridging B-H-Si site, while Raman studies by Stutzmann[32] have provided evidence for direct B-H pair formation in crystalline silicon. IR and annealing studies by Berman *et al.*[33] have also shown the formation of donor-H complexes. They have, however, inferred that the hydrogen is not directly associated with the donor atoms and the concentration of the complexes decreases upon annealing. The average distance between this segregated bulk hydrogen would then depend on the boron concentration. The average distance between boron atoms is $\sim$19 Å and $\sim$50 Å in samples 1 and 2, respectively. Since MQ NMR experiments typically probe distances between 10–20 Å, the hydrogen in the bulk of sample 1 is picked up in addition to the hydrogen in the voids. Though this hydrogen would participate in the MQ transition (particularly at long values of τ), it would have little effect on $N(\tau)$, which would be determined by clustered hydrogen in microvoids where the distance between the spins is less than 20 Å. Comparing the value of $M_{\rm sat}$ with that of f_B, it is evident that the fraction of hydrogen contributing to the broad line is approximately half that of hydrogen participating in the MQ transitions

in sample 1. Upon annealing, the concentration of impurity-H complexes is expected to decrease[32] and M_{sat} in sample 1 decreases slightly to ~ 0.75. The "size" of the hydrogen clusters, however, remains unchanged, indicating that the flat microvoids can accommodate about ten hydrogen atoms.

In sample 2, the situation is somewhat different. With the average distance between boron atoms ~ 50 Å, MQ NMR experiments can only "see" hydrogen atoms that are in close proximity to each other. Upon annealing one of two things might be happening. The microvoid surfaces may become increasingly hydrogenated due to diffusion of hydrogen. Note that these microvoids can only accommodate approximately ten atoms. This would imply that $N(\tau)$ would change with annealing. Since the error bars associated with each data point are at least ± 1 spins, and the changes are small, the data remain ambiguous. The other possibility is that the number of microvoids in this sample increases upon annealing, while the average number of hydrogen atoms trapped in these voids remains approximately the same. In either case, both M_{sat} and $I(n)$ $(n \geq 2)$ would increase, reflecting these changes, although the distance between the clusters would be different in the two cases.

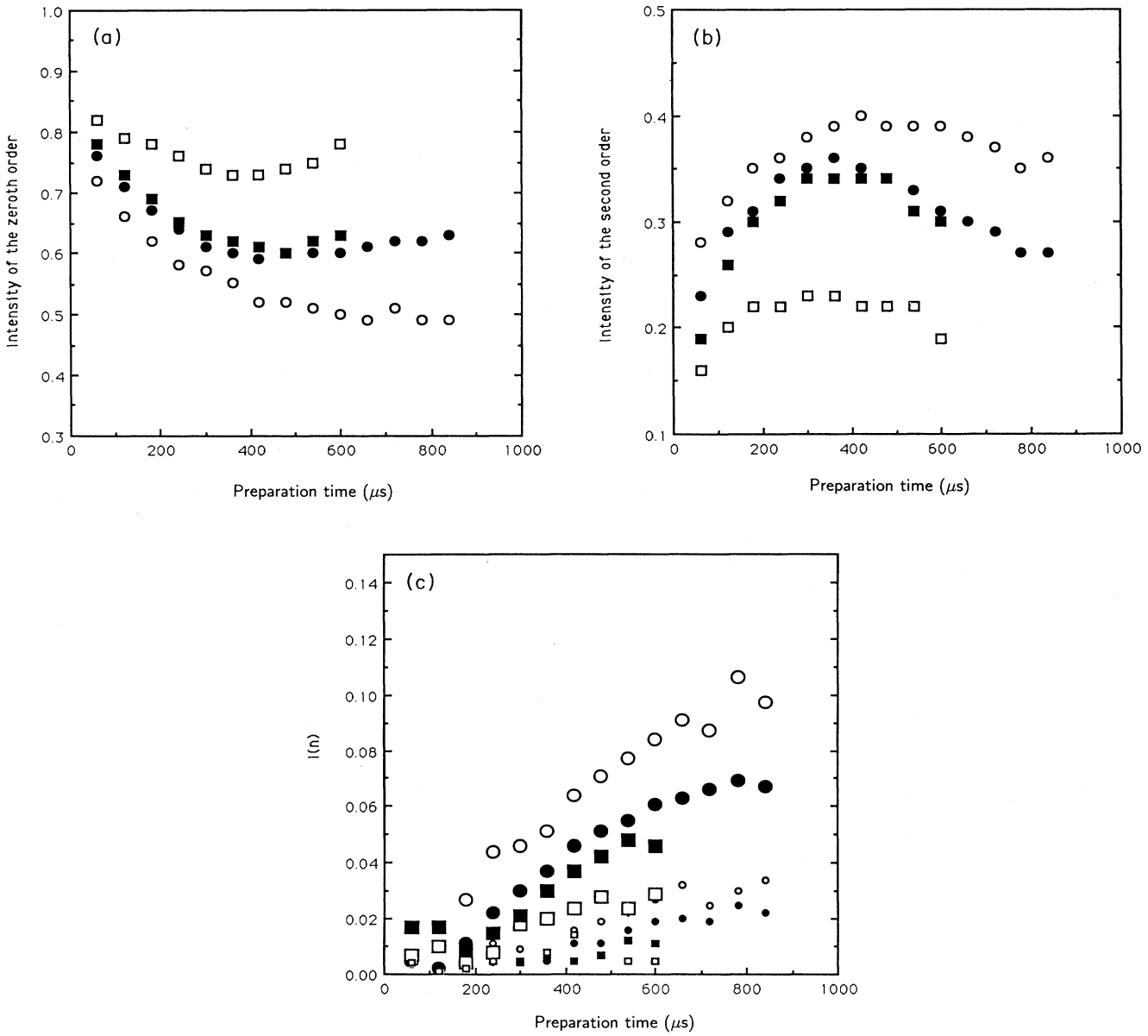

FIG. 7. Dependence of the normalized (a) $I(0)$, (b) $I(2)$, and (c) higher orders on preparation time for samples 1 (circles) and 2 (squares) both before (open symbols) and after annealing (solid symbols). The larger and smaller symbols in part (c) represent $I(4)$ and $I(6)$, respectively.

IV. CONCLUSIONS

We have studied the effect of boron doping on hydrogen microstructure in rf-sputter-deposited *a*-Si:H using IR absorption and ^{1}H NMR. We have shown that for as-deposited boron-doped films the hydrogen microstructure depends on the boron concentration. The hydrogen microstructure, as determined by ^{1}H MQ NMR, is clearly different in the two doped samples. In sample 2, where the only hydrogen IR stretch frequency occurs at 2000 cm^{-1}, MQ transitions are important. Upon annealing the fraction of clustered hydrogen in this sample increases, though there is no discernible change in its IR spectra. Thus there are hydrogen atoms which are in close proximity to each other so that dipole-dipole interactions are important, yet experience dielectric screening similar to that in the bulk.

These results are consistent with the model of flat disks as deep trapping sites for hydrogen. We have also shown conclusively that even moderate annealing leads to changes in the hydrogen microstructure. Note that there is a close match between the values of M_{sat}, f_B, and $N(\tau)$ in both samples after annealing. This is not surprising since both samples have similar contents of hydrogen and are expected to relax to a similar state.

ACKNOWLEDGMENTS

We would like to thank Dr. Ruth Shinar for determining the boron content of the films using SIMS. This work was supported in part by NSF Grant No. CTS-9057119. Ames Laboratory is operated by the Iowa State University for the U.S. Department of Energy under Contract No. W-7405-Eng-82.

*Author to whom correspondence should be addressed.

[1]A. Matsuda, M. Matsumura, K. Nagiakgaqwa, T. Imura, H. Yamanoto, S. Yamusaki, H. Okushi, S. Iizima, and K. Tananaka, in *Tetrahedrally Bonded Amorphous Semiconductors,* edited by R. A. Street, D. K. Biegelson, and J. C. Knights (American Institute of Physics, New York, 1981), p. 192.

[2]Y. Hamakawa and H. Okamoto, in *Advances in Solar Energy,* edited by K. W. Boer (Plenum, New York, 1989), Vol. 5, p. 1.

[3]P. G. Lecomber, J. Non-Cryst. Solids **115**, 1 (1989).

[4]D. L. Staebler and C. R. Wronski, Appl. Phys. Lett. **31**, 292 (1977).

[5]C. R. Wronski, in *Semiconductors and Semimetals,* edited by J. I. Pankove (Academic, Orlando, 1984), Vol. 21C, p. 347.

[6]S. Mitra, Ph.D. thesis, Iowa State University, 1991.

[7]D. E. Carlson and C. W. Magee, Appl. Phys. Lett. **33**, 81 (1978).

[8]E. Bhattacharya and A. H. Mahan, Appl. Phys. Lett. **52**, 1587 (1988).

[9]S. Zafar and E. A. Schiff, Phys. Rev. B **40**, 5235 (1989).

[10]S. Zafar and E. A. Schiff, Phys. Rev. Lett. **66**, 1493 (1991).

[11]W. E. Carlos and P. C. Taylor, Phys. Rev. B **26**, 3605 (1982).

[12]J. A. Reimer, Phys. Rev. Lett. **56**, 1377 (1986).

[13]J. A. Reimer, R. W. Vaughan, and J. C. Knights, Phys. Rev. B **23**, 2567 (1981); **24**, 3360 (1981).

[14]K. K. Gleason, M. A. Petrich, and J. A. Reimer, Phys. Rev. B **36**, 9722 (1987).

[15]M. A. Petrich (unpublished).

[16]J. Shinar, R. Shinar, S. Mitra, and J.-Y. Kim, Phys. Rev. Lett. **62**, 2001 (1989).

[17]S. Mitra, D. H. Levy, K. K. Gleason, H. Jia, and J. Shinar, in *Amorphous Silicon Technology–1992,* edited by M. J. Thompson, Y. Hamakawa, P. G. LeCombra, A. Madan, and E. A. Schiff, MRS Symposia Proceedings No. 258 (Materials Research Society, Pittsburgh, 1992), p. 269.

[18]M. Cardona, Phys. Status Solidi B **118**, 463 (1983).

[19]A. H. Mahan, D. L. Williamson, B. P. Nelson, and R. S. Crandall, Phys. Rev. B **40**, 12 024 (1989).

[20]H. R. Shanks, F. R. Jeffrey, and M. E. Lowry, J. Phys. (Paris) Colloq. **42**, C4-773 (1981).

[21]H. Fritzsche and X.-M. Deng, Bull. Am. Phys. Soc. **35**, 349 (1990).

[22]S. Mitra, R. Shinar, and J. Shinar, Phys. Rev. B **42**, 6746 (1990).

[23]J. Baum, K. K. Gleason, A. N. Garroway, and J. A. Reimer, Phys. Rev. Lett. **56**, 1377 (1986).

[24]S. LaCelle, Adv. Magn. Res. **16**, 173 (1991).

[25]K. K. Gleason, Concepts Magn. Res. (to be published).

[26]H. R. Shanks, C. J. Fang, L. Ley, M. Cardona, F. J. Demond, and S. Kablitzer, Phys. Status Solidi B **100**, 43 (1980).

[27]E. Fukushima and S. B. W. Roeder, *Experimental Pulse NMR: A Nuts and Bolts Approach* (Addison-Wesley, Reading, MA, 1981), p. 168.

[28]M. S. Conradi and R. E. Norberg, Phys. Rev. B **24**, 2285 (1981).

[29]D. H. Levy and K. K. Gleason, J. Phys. Chem. **96**, 8125 (1992).

[30]R. A. Street, C. C. Tsai, J. Kakalios, and W. B. Jackson, Philos. Mag. B **56**, 305 (1987).

[31]J. I. Pankove, P. J. Zanaucchi, C. W. Magee, and G. Lucovsky, Appl. Phys. Lett. **46**, 421 (1985).

[32]M. Stutzmann, Phys. Rev. B **35**, 5921 (1987).

[33]K. Bergman, M. Stavola, S. J. Pearton, and J. Lopata, Phys. Rev. B **37**, 2770 (1988).